CAMS Service Evolution

D1.5 Report on 1-year 3MI proxy data: delivery of the conventional retrievals and retrievals adapted for the aerosol representation CAMS

Due date of deliverable	30/06/2024
Submission date	12/08/2024
File Name	CAMEO-D1.5-V1.1
Work Package /Task	Global aerosol assimilation in CAMS/ T1.2 Adaptation of aerosol parameter retrievals from 3MI, MAP/CO2M, S-3, -4,-5P and other instruments for the aerosol representation in CAMS (global)
Organisation Responsible of Deliverable	LOA, GRASP-SAS
Author name(s)	Oleg Dubovik, Pavel Litvinov, Milagros Herrera, Christian Matar, Marcos Herreras
Revision number	V1.1
Status	Issued
Dissemination Level	Public

Funded by the European Union

The CAMEO project (grant agreement No 101082125) is funded by the European Union.
Views and opinions expressed are however those of the author(s) only and do not necessarily reflect those of the European Union or the Commission. Neither the European Union nor the granting authority can be held responsible for them.

Table of Contents

1 Scope of the deliverable

This document provides the three data sets of aerosol products derived from POLDER-3/PARASOL observations that considered as proxy 3MI observations. The first data set represents conventional aerosol products that includes all retrieved parameters containing extended set of the detailed optical properties of aerosol and surface properties. For example, the aerosol product includes spectral aerosol optical depth (AOD), fine mode AOD (AODF) and coarse mode AOD (AODC), spectral aerosol absorption optical depth (AAOD), single scattering albedo (SSA), as well as, Ångström exponent (AE). It should be noted that these data provide significantly more complete description of aerosol properties compare to popular MODIS product that include mainly data of total AOD, while other parameters such as AE are not reliable, especially over land, compared to AE provided by POLDER-3/GRASP (Chen et al., 2020).

The second data set is provided as an illustration of new approach of aerosol remote sensing retrieval that is more adapted for the aerosol representation aerosol climate models, especially in CAMS. The concept of approach and details of main activities, in the frame of CAMEO project, aimed on further harmonization of aerosol remote sensing retrieval with CAMS are presented and described in details in D1.4 “Report on aligning aerosol parameter retrievals” (Litvinov et al., 2024). The approach relies on new “GRASP/Components” concept (Li et al., 2019, 2020a,b). In the frame of this concept the complex refractive index of aerosol is not derived directly as in AERONET retrieval (Dubovik and King, 2000, Dubovik et al., 2000, 2006) or POLDER-3/GRASP-HP approach (Chen et al., 2020), instead the aerosol is represented as a mixture of different aerosol components with predefined spectral complex refractive index, and therefore the retrieved fractions drive the aerosol spectral index of refraction of total aerosol. In addition, fraction of spherical particles and the aerosol layer height (ALH) are also included in state vector of retrieval aerosol parameters. The aerosol vertical distribution was modeled using an exponential profile and scale height was retrieved.

After number of tests, a new “GRASP/Components” approach (Li et al., 2019, 2020a,b) has been adapted for implementation for 3MI operation and it was extensively applied to 3MI proxy POLDER-3 data. The entire archive of POLDER-3 data was processed using GRASP/Components and extensively validated (Zhang et al., 2021). The results are available at https://www.grasp-open.com/products/. In this deliverable we provide later processing of POLDER-3 data with improved definition of aerosol components that allow further improvements in the retrieval of aerosol optical properties such as AOD, AE, SSA, etc.

Finally, we added data set of the POLDER-3 processing generated using GRASP/Components with the latest version of aerosol model representation. In difference with previous version, this processing retrieves two externally mixed aerosol modes: fine mode, coarse desert dust, and coarse sea salt. In This approach, in a contrast with previous retrieve different size distributions for desert dust and sea salt aerosol coarse modes of aerosol. As shown in D1.4 (Litvinov et al., 2024) this configuration of aerosol retrieval allows some improvements in retrieved aerosol properties. At the same time, this GRASP aerosol retrieval configuration is closer to aerosol representation in CAMS. It should be noted however, that since this configuration is planned to improved further in CAMEO studies, the processing was done globally but only over AERONET sites.

1.1 Objective of the deliverable and work performed

Several extensive data sets of the retrieval products from 3mMI/Proxy POLDER-3 data were prepared in user friendly format and made available for CAMEO and general broad scientific community. The objective of these efforts it to provide an example of advanced aerosol retrieval product that could be used by the community for investigating and the qualitative and quantitative differences in aerosol products to be available from new multi-angular polarimetric (MAP) missions, such as 3MI/EPS-SG, MAP/CO2M, HARP-2 and SPEX/PACE, etc. Moreover, these data set and this report are prepared in specific manner that has several rather strategic complementary objectives to:

- *to demonstrate* the value of new detailed MAP products providing extensive set of detailed aerosol optical properties: AE, spectral AODF, AODC, SSA, AAOD, etc.;
- *to demonstrate* the potential of MAP satellite product to provide information about not only amount of aerosol but also on variability of its composition;
- *to demonstrate* a possibility of close aligning assumptions in aerosol remote sensing approaches using processing MAP observation and chemical transport models (CTM);
- *to demonstrate* the idea of above aligning aerosol modelling in remote sensing with CTM and *to outline* very promising strategic direction of aerosol remote sensing evolution that bring double complementary benefits of:
    - *improving **efficiency of** satellite **aerosol product assimilation** into CTM;*
    - *improving **scope and accuracy of aerosol optical properties** retrieved from remote sensing.*

Specifically, the first POLDER/Models data set provides the extended set of aerosol MAP products that provide base satellite product AOD (that was already available, e.g. from MODIS) of similar of higher accuracy than from conventional MODIS product together with advanced aerosol products : AE, AODF, AODC, SSA, AAOD that generally are not available from other conventional (not MAP) satellite. The second GRASP/components data set provides similar set of aerosol optical parameters, while they were derived using conceptually different POLDER/components retrieval approach. It derives the size resolved fractions of aerosol components representing different aerosol composition species, such as black carbon, brown carbon, fine/coarse mode non-absorbing soluble and insoluble, coarse mode absorbing and aerosol water. The retrieved fractions drive the aerosol spectral index of refraction in modelling of atmospheric radiances. As a result, this data set includes not only parameters characterizing distribution of the aerosol optical parameters and also parameters suggesting aerosol composition such as volume factions of carbon, brown carbon, etc. This shows that aerosol representation of aerosol microphysics and composition in POLDER/components approach is close to that in CTMs. At the same time, as will be discussed below, the analysis shows that POLDER/components approach provides the entire set of aerosol optical properties (AOD, AE, AODF, AODC, SSA, AAOD) that is overall more consistent and even more accurate than provided by POLDER/Models approach designed as direct retrieval optical aerosol parameters.

Finally, the last data set provides examples of aerosol retrieval obtained using POLDER/components approach modified in frame of CAMEO project. These modifications were suggested in the frame of this CAMEO project (see detailed discussion in D1.4, Litvinov et al., 2024) with the aim of achieving further harmonization of aerosol description in remote sensing and CTM. It was shown the suggested modifications not allowed two positive outcomes: (i) to make model of aerosol used in remote sensing closer to that of CTM and (ii) to provide all aerosol optical properties with the same and even higher accuracy than earlier version of POLDER/components approach. The later conclusion suggests high potential of further efforts in aligning and harmonization of aerosol modelling in remote sensing and CTMs.

1.2 Aerosol optical properties provided from 3MI Proxy retrievals

The MAP observations are considered as the most promising type of passive satellite observation and several new polarimetric missions are deployed or planned to be deployed in the near future (Dubovik et al., 2019). The extensive efforts by Dubovik et al. (2011, 2014, 2021), Li et al., (2019, 2020a,b), Chen et al.(2020), Hasekamp et al. (2024) demonstrated the full real potential of MAP retrieval to provide rather complete and accurate set of aerosol optical parameters together with some inside of aerosol composition. The delivered data set can be used by CAMEO team and general community to test the products and use for different comparisons and applications. The additional useful information about each data set is provided in the this section.

1.2.1 Advanced optical properties of aerosol products generated from multi-angular polarimetric observations

The first POLDER/Modes data set can be used to demonstrate the aerosol product that provide base AOD aerosol product of similar or higher accuracy compared to conventional MODIS product together with advanced (AE, AODF, AODC, SSA, AAOD) that practically not available from conventional observations as those from MODIS. At the same time, it should be noticed that this is not the first version of aerosol product derived from POLDER observations.

Initially, the full POLDER-3 data archive was processed by GRASP using the three following retrieval configurations: POLDER-3/GRASP «optimized», «high-precision», «models» and «components» approaches. The «optimized» and «high-precision» are designed as AERONET-like retrieval (Dubovik and King, 2000, Dubovik et al., 2006) where the retrieved state vector includes size distribution together with values spectral index of refraction and faction of spherical particles. In addition, the aerosol scale height was retrieved too (Dubovik et al., 2011). The «optimized» and «high-precision» differ between themselves only by the precision of the RT calculations. The «models» approach uses the assumption of an external mixture of several aerosol components and directly retrieved parameters including aerosol concentrations and a scale height (Chen et al., 2020, Dubovik et al., 2021). The retrieval data products of all approaches contain the aerosol main aerosol characteristics including spectral AOD, AAOD, SSA as well as AE, spectral AODF and AODC. All these products were extensively evaluated using validations against AERONET and comparisons with the original POLDER algorithm (PARASOL/Operational), and MODIS Collection 6 aerosol products (Chen et al., 2020). The detailed validation was performed for Level 3 to 0.1 degree products. The studies have shown that the POLDER-3/GRASP retrievals provided reliable aerosol products. Specifically, POLDER-3/GRASP spectral products including AOD for six wavelengths in the range 443 to 1020 nm agree well with the AERONET AOD measurements, e.g. for POLDER-3/Models AOD correlation coefficients R are ≥ 0.86 over land and ≥ 0.94 over ocean with BIAS not exceeding 0.01 over land and 0.02 over ocean for all wavelengths. The upper panel of Fig. (1) demonstrates the correlations of satellite AOD with AERONET for several selected wavelengths.

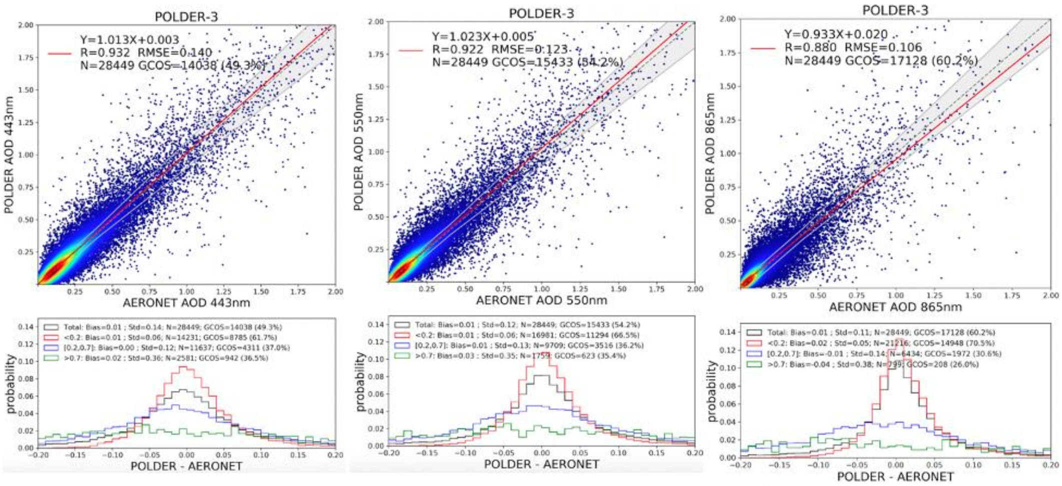

Figure 1: The illustrations of the POLDER/GRASP product comparisons with AERONET data: the correlations of POLDER-3/Models AOD with AERONET for several selected wavelengths (440, 550, 870 nm) for entire POLDER archive.

The comparisons with MODIS aerosol products showed that the POLDER-3/GRASP AOD retrievals are very coherent with popular MODIS data and POLDER/Operational while also exhibiting some advancements. For example, Fig. (2) shows that over ocean the POLDER/Models AOD retrievals are fully coherent with MODIS globally over ocean. Moreover, the validations against AERONET both over ocean and land, shown on Figs. (1-2) suggest that POLDER/Models have somewhat superior accuracy over MODIS and POLDER/Operational AOD products.

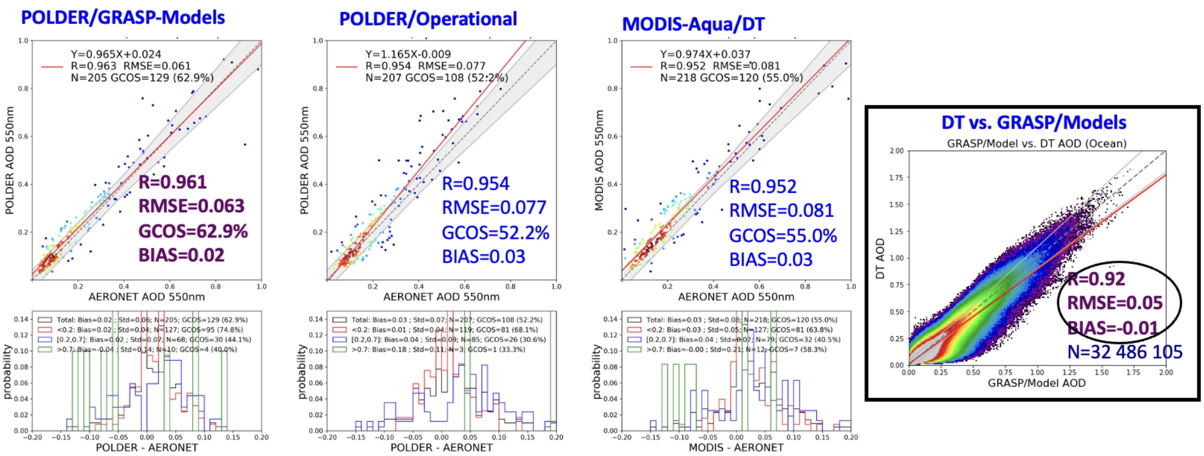

Figure 2: From left to right: The illustrations of the POLDER/Models, POLODER/Operational and MOIDIS/DT products comparisons with AERONET data over ocean for year 2008, and global pixel to pixel comparison of MOIDIS/DT and POLDER/Models AOD over ocean for year 2008.

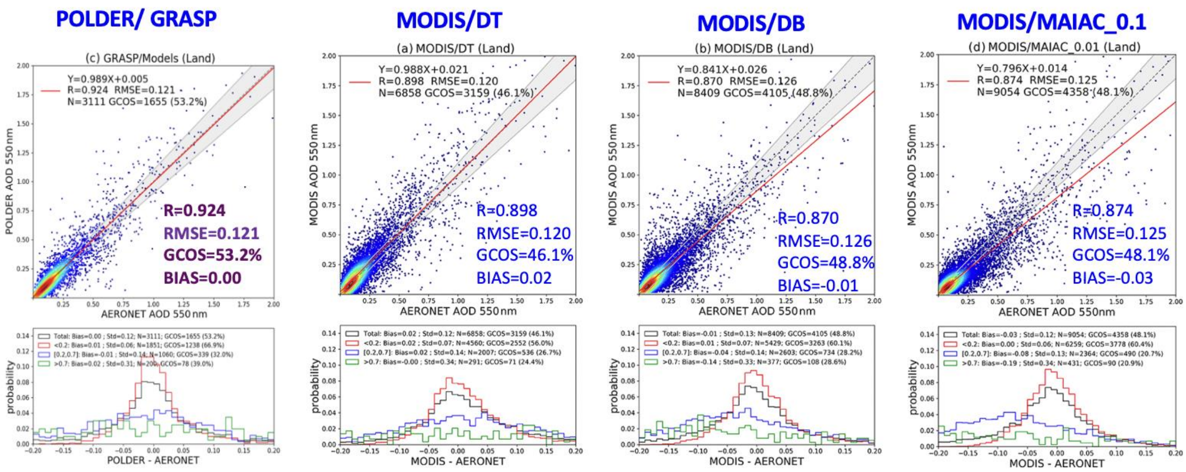

Figure 3: From left to right: the illustrations of the POLDER/Models MOIDIS/DT, MOIDIS/DB and MOIDIS/MAIAC products comparisons with AERONET data over land for year 2008.

The comparisons with MODIS manifested clear advantages of POLDER product in providing more reliable detailed aerosol parameters such as AE, AODF and AODC especially over land and such parameters as SSA and AAOD that are generally not available from MODIS-like instruments, while the validation of POLDER-3/GRASP products by Chen et al., (2020) showed a robust correlation of the retrieved SSA and AAOD spectral values with AERONET (440–1020 nm), correlations increase for the retrievals corresponding to the events with higher AOD. For AAOD retrievals overall the bias did not exceed 0.01, suggesting that POLDER-3/GRASP products can be used for making global estimations of AAOD at such a level of uncertainty. Figure 4 demonstrates the correlations of the detailed POLDER-3/GRASP products.

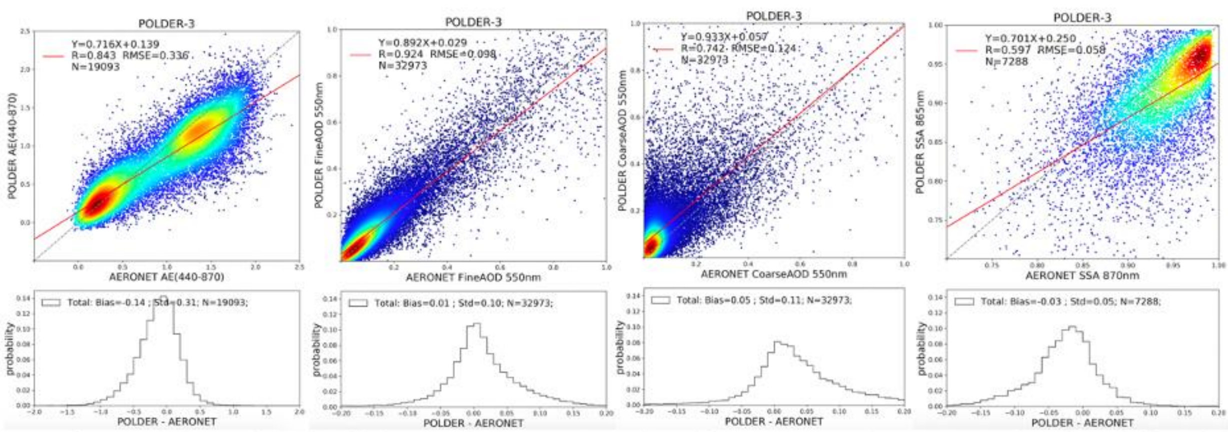

Figure 4: The illustrations of the POLDER/GRASP product comparisons with AERONET data: the correlations of the detailed aerosol parameters retrieved by POLDER-3/GRASP/HP product, from left to right: AE, AODF(550), AODC(550), SSA(865).

Thus, the analysis showed that in terms of AOD that characterize total amount aerosol MAP retrieval show comparable or even somewhat better capabilities compared to conventional MODIS retrieval, while MAP products seem to be significantly more capable in characterizing detailed properties of aerosol related with difference in type of aerosol particles. This advantage is illustrated by illustrations provided by Fig. (5). One can see that monthly maps of AOD obtained from MODIS and POLDER are rather coherent and do not manifest evident difference. In contrast, the monthly maps of AE from MODIS and POLDER are significantly different, where AE from MODIS show some unrealistic patterns. For example, smoke originated from well-known biomass burning outbreak in central Africa is characterized by very different AE over land (rather high) and ocean (quite low). This anomaly results in shown evidently false significant values of AODC in transported smoke (lower panel in Fig.(5). POLDER/GRASP retrieval of AOD, AE and AODC seem to be rather consistent over land and ocean.

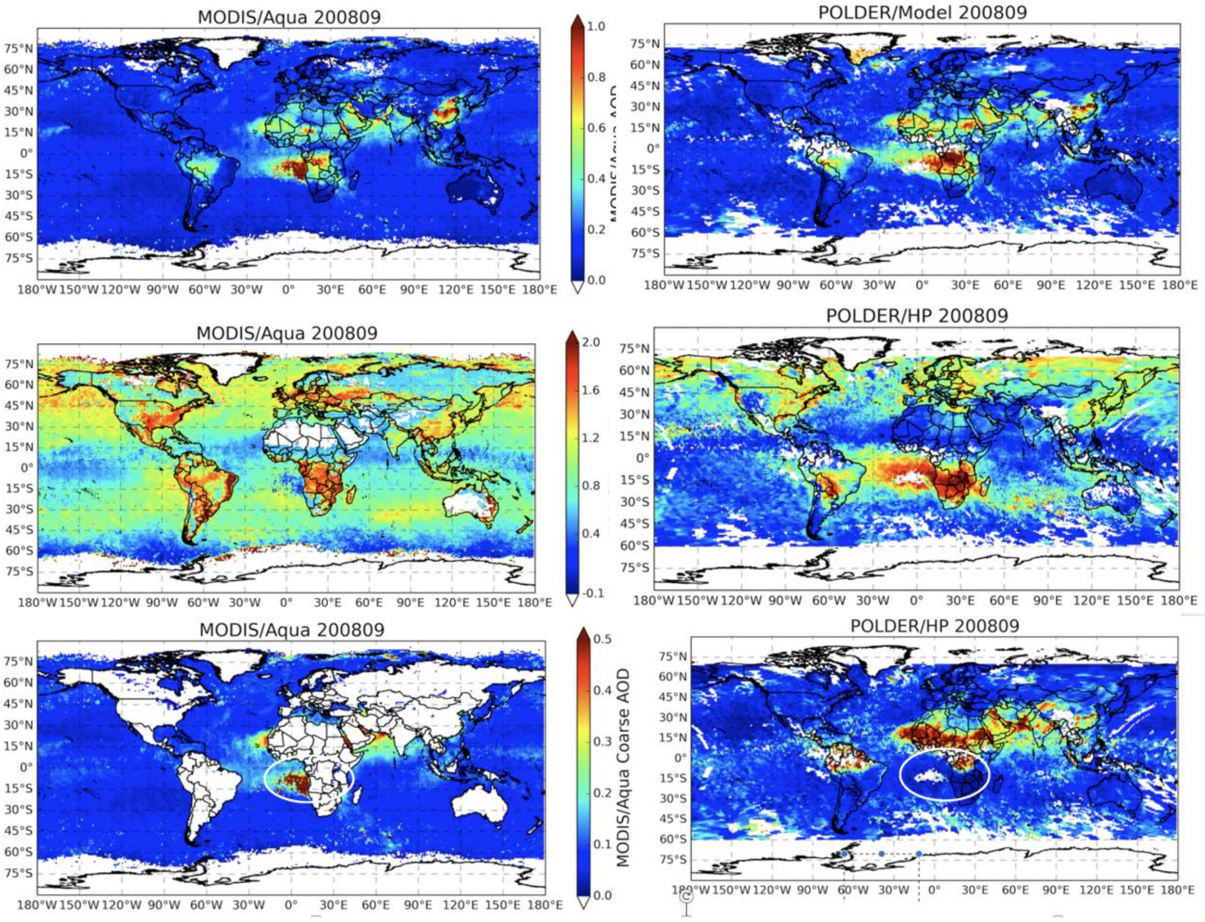

Figure 5: The monthly averaged AOD (top), AE (middle) and AODC (bottom) for September 2008 provided from MODIS/DT (left) and POLDER/GRASP products (right).

One of very important findings of Chen et al., (2020) analysis is that the best retrieval of total AOD was provided by the simplest approach (GRASP/Models). This is reason why GRASP/Models provided as first data set in the present deliverable. The more complex approaches GRASP/HP and GRASP/Optimized over land had notable bias (~0.06 - 0.07 at 500) as can be seen from Table 1.

In GRASP/Models the retrieval is restrained to a superposition of predefined aerosol components, significantly reducing the number of free parameters for retrieval. The more complex GRASP/HP retrieval with more retrieval parameters seemed to provide more accurate detailed aerosol parameters such as AE, AODF, AODF and SSA. Indeed, multi-angular polarimetric observations have sensitivity to different aerosol properties, and therefore the MAP algorithms tend to be designed for the retrieval of large number of parameters, while in the situations with low aerosol presence the information from observations may not be sufficient to retrieve all parameters reliably. Evidently, Chen et al., (2020) analysis concluded that future efforts on improving the POLDER-3/GRASP retrieval showed be aimed at achieving accurate retrievals within one approach, however the situation also reveals the challenge of developing a unique approach that can provide a retrieval of all parameters with highest accuracy from MAP observations. In these regards the later approach - GRASP/Components provided apparently the most coherent total and detailed aerosol properties. The validation against AERONET of the first product generated POLDER/Components properties by Zhang et al., (2021) showed that this approach apparently provides the most coherent total and detailed aerosol properties. Specifically, the accuracy of total AOD from GRASP/Components is higher than AOD form GRASP/HP and GRASP/Optimized and close to GRASP/Models, while most of detailed aerosol product (AODF, AODC, AE,) higher or close to the best results of GRASP/HP and GRASP/Optimized. This issue was additionally thoroughly investigated in the frame of ESA HARPOL project (https://eo4society.esa.int/projects/harpol/) where the two algorithms GRASP and RemoTAP (Hasekamp et al., 2011; Fu and Hasekamp, 2018) were thoroughly compared using benchmark theoretical computations and applications to real POLDER-3 data (Hasekamp et al., 2024). The strengths and weaknesses were identified and the effort to find the best approaches and to improve the algorithms were undertaken. The similar issue was identified in an earlier version of RemoTAP algorithm in which a large number of unknowns was also retrieved. Finally, it was shown in Hasekamp et al. (2024) that rather accurate retrieval with no essential biases of AOD and detailed characteristics such as AE, AODF, AODC, etc. could obtained using all approaches including «optimized» and «high-precision» by moderate decreasing the number of retrieved parameters. Nonetheless, POLDER/Components approach was recognized as overall most practically efficient approach allowing accurate retrieval of both AOD and detailed aerosol properties.

Land/ocean	Band (nm)	Products	R	Slope	Offset	RMSE	GCOS (%)	Bias	Bias $\tau < 0.2$	Bias $0.2 \le \tau \le 0.7$	Bias $\tau > 0.7$
Land	443	Optimized (41268)	0.900	0.867	0.104	0.179	26.7	0.06	0.09	0.06	−0.06
		HP (42202)	0.915	0.981	0.072	0.181	32.7	0.07	0.07	0.07	0.05
		Models (28449)	**0.932**	**1.013**	**0.003**	**0.140**	**49.3**	**0.01**	**0.01**	**0.00**	**0.02**
	490	Optimized (41268)	0.892	0.879	0.099	0.171	26.8	0.06	0.08	0.06	−0.04
		HP (42202)	0.909	**1.000**	0.069	0.174	33.2	0.07	0.07	0.07	0.07
		Models (28449)	**0.929**	1.025	**0.003**	**0.131**	**51.6**	**0.01**	**0.01**	**0.01**	**0.03**
	550	Optimized (41268)	0.876	0.847	0.101	0.162	27.5	0.06	0.08	0.05	−0.08
		HP (42202)	0.898	0.973	0.074	0.163	34.0	0.07	0.07	0.07	0.04
		Models (28449)	**0.922**	**1.023**	**0.005**	**0.123**	**54.2**	**0.01**	**0.01**	**0.01**	**0.03**
	565	Optimized (41268)	0.877	0.877	0.096	0.161	27.3	0.06	0.08	0.06	−0.05
		HP (42202)	0.898	**1.004**	0.069	0.165	34.0	0.07	0.07	0.07	0.07
		Models (28449)	**0.920**	1.011	**0.006**	**0.120**	**54.4**	**0.01**	**0.01**	**0.00**	**0.02**
	670	Optimized (41268)	0.858	0.823	0.099	0.152	28.4	0.06	0.08	0.05	−0.10
		HP (42202)	0.886	**0.955**	0.077	0.153	35.0	0.07	0.07	0.07	**0.02**
		Models (28449)	**0.911**	0.954	**0.016**	**0.108**	**58.6**	**0.01**	**0.01**	**−0.01**	−0.03
	865	Optimized (41268)	0.816	0.785	0.093	0.142	31.3	0.05	0.07	0.03	−0.15
		HP (42202)	0.856	0.932	0.074	0.142	37.6	0.06	0.06	0.07	**−0.02**
		Models (284449)	**0.880**	**0.935**	**0.018**	**0.105**	**60.3**	**0.01**	**0.02**	**−0.01**	−0.04
	1020	Optimized (40148)	0.791	0.772	0.089	0.139	32.8	0.05	0.07	0.02	−0.17
		HP (41016)	0.837	0.924	0.073	0.138	38.8	0.06	0.06	0.06	**−0.03**
		Models (27551)	**0.856**	**0.943**	**0.023**	**0.109**	**59.5**	**0.01**	**0.02**	**0.00**	−0.04
Ocean	443	Optimized (1495)	0.938	**1.028**	0.049	0.084	40.5	0.05	0.05	0.07	**0.03**
		HP (1551)	0.939	1.043	0.046	0.083	41.2	0.05	0.05	0.06	0.05
		Models (2064)	**0.940**	0.970	**0.026**	**0.066**	**60.6**	**0.02**	**0.02**	**0.03**	−0.06
	490	Optimized (1495)	0.939	1.064	0.041	0.079	43.2	0.05	0.04	0.07	**0.05**
		HP (1551)	0.942	1.077	0.039	0.079	43.1	0.05	0.05	0.07	0.09
		Models (2064)	**0.946**	**0.969**	**0.023**	**0.057**	**65.1**	**0.02**	**0.02**	**0.02**	**−0.05**
	550	Optimized (1495)	0.936	1.060	0.035	0.071	48.4	0.05	0.04	0.06	**0.04**
		HP (1551)	0.940	1.083	0.036	0.074	46.4	0.05	0.04	0.07	0.11
		Models (2064)	**0.950**	**0.960**	**0.019**	**0.050**	**70.3**	**0.01**	**0.01**	**0.01**	−0.05
	565	Optimized (1495)	0.939	1.090	0.033	0.072	48.5	0.05	0.04	0.07	**0.05**
		HP (1551)	0.943	1.105	0.033	0.074	46.7	0.05	0.04	0.07	0.12
		Models (2064)	**0.950**	**0.939**	**0.020**	**0.048**	**71.2**	**0.01**	**0.01**	**0.00**	−0.07
	670	Optimized (1495)	0.936	**1.071**	0.030	0.064	55.8	0.04	0.04	0.06	**0.02**
		HP (1551)	0.943	1.099	0.032	0.068	50.9	0.05	0.04	0.07	0.11
		Models (2064)	**0.951**	0.876	**0.021**	**0.043**	**77.3**	**0.00**	**0.01**	**−0.02**	−0.13
	865	Optimized (1495)	0.931	**1.077**	0.020	0.053	66.0	0.03	0.03	0.05	0.15
		HP (1551)	0.942	1.129	0.024	0.060	58.3	0.04	0.03	0.06	0.17
		Models (2064)	**0.955**	0.852	**0.015**	**0.038**	**82.1**	**0.00**	**0.00**	**−0.03**	**−0.13**
	1020	Optimized (1431)	0.927	**1.063**	0.017	0.049	71.3	0.02	0.02	0.04	0.15
		HP (1501)	0.940	1.143	0.021	0.058	60.9	0.04	0.03	0.07	0.18
		Mod[illegible]	**[illegible]57**	0.865	**0.013**	**0.035**	**84.6**	**0.00**	**0.00**	**−0.03**	**−0.11**

Table 1: Global statistics of PARASOL/GRASP spectral AOD vs. AERONET AOD over land and ocean. The best performing of three approaches by each metric is labelled in bold (adapted from Chen et al., 2020).

As a result, GRASP/Components (same as RemoTAP) algorithm was significantly improved during the HARPOL project. Additionally, further improvement of GRASP/Components were done within CAMEO studies. It should be noted that the most advanced POLDER/RemoTAP approach uses rather similar aerosol modeling concept to one of GRASP/components. Specifically, GRASP uses a somewhat slightly optimized GRASP/Components approach compared to Li et al., (2019), and the RemoTAP approach also represents aerosol using several externally mixed aerosol components with predetermined complex refractive index while description of size distribution and other parameters of each component is somewhat different.

Figure 6 illustrates the validation results of the retrieved aerosol parameters by the latest global processing using GRASP/Components, that provided as a second data set in frame of this deliverable).

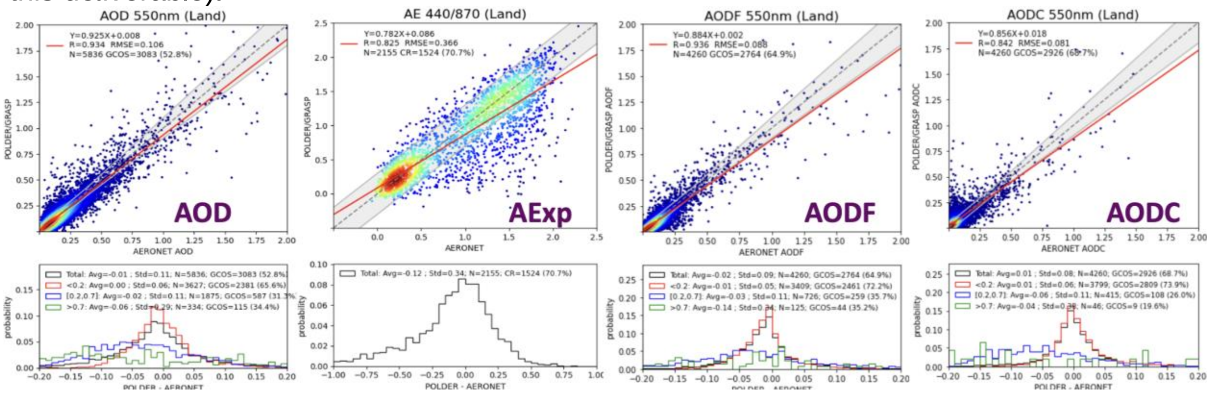

Figure 6: The results of validation of 1-year 2008 POLDER-3/Components latest global product provided as second 3MI/Proxy aerosol product.

It can be again emphasized here that POLDER validation statistics are rather convincing especially compared with conventional aerosol retrieval as those from single view imagers such as MODIS in particular for so-called detailed parameters (e.g., AE and AODF). In addition to the illustration of Fig.(5), Fig. (7) shows the global validation of MODIS AE and comparison with POLDER AE over land. One can see that POLDER AE shown is significantly more accurate than MODIS AE. This becomes evident in particular from the global pixel-to-pixel comparisons of MODIS AE to POLDER AE where it is made evident that MODIS AE is relying on the predetermined aerosol presumably regional aerosol models and doesn’t capture local variation of AE.

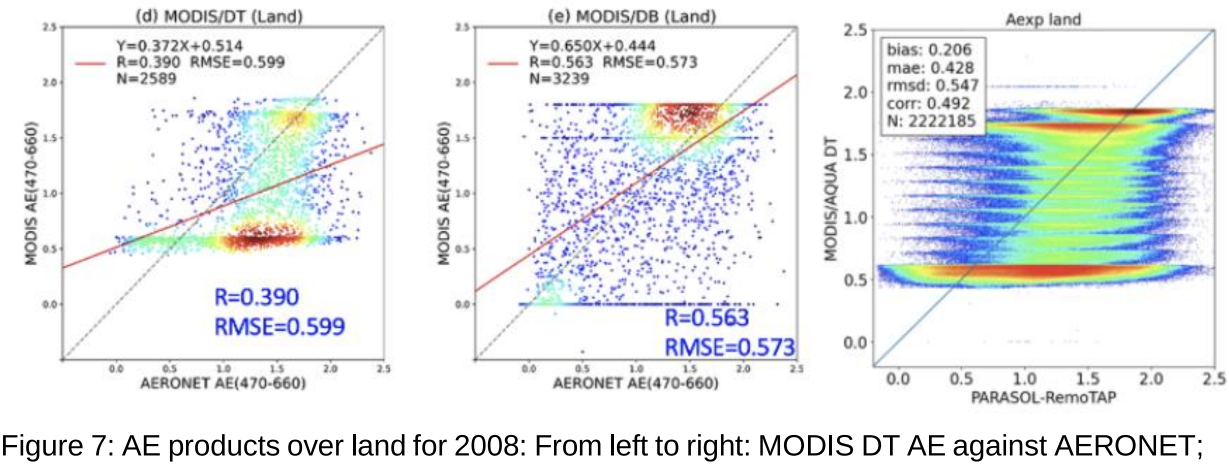

Figure 7: AE products over land for 2008: From left to right: MODIS DT AE against AERONET; MODIS DB AE against AERONET, global comparison of MODIS DT AE against POLDER RemoTAP AE (adapted from Hasekamp et al., 2024).

The version of GRASP/Components retrieved updated with the finding from HAPRPOL studies and few more improvement was used for generation of POLDER/Components retrieval provided in this deliverable.

1.2.2 Aerosol composition information provided by 3MI Proxy retrievals based on aerosol assumption harmonized with CTMs.

As discussed in previous section the concept of GRASP/Components approach seems to be very useful for optimizing scope and accuracy of aerosol optical properties (AOD, AODF, AODC, SSA and AAOD). At the same time, the initial idea of this approach was related mostly with a possibility to provide directly some information about aerosol composition. Indeed, the GRASP/components approach retrieves the size resolved fractions of aerosol components representing the different species, such as black carbon, brown carbon, fine/coarse mode non-absorbing soluble and insoluble, coarse mode absorbing and aerosol water (Li et al., 2019). For example, Fig.(8) illustrates the climatology of aerosol component columnar mass concentration derived from POLDER-3 over the East Asia region by the GRASP/Components algorithm (Li et al., 2020b).

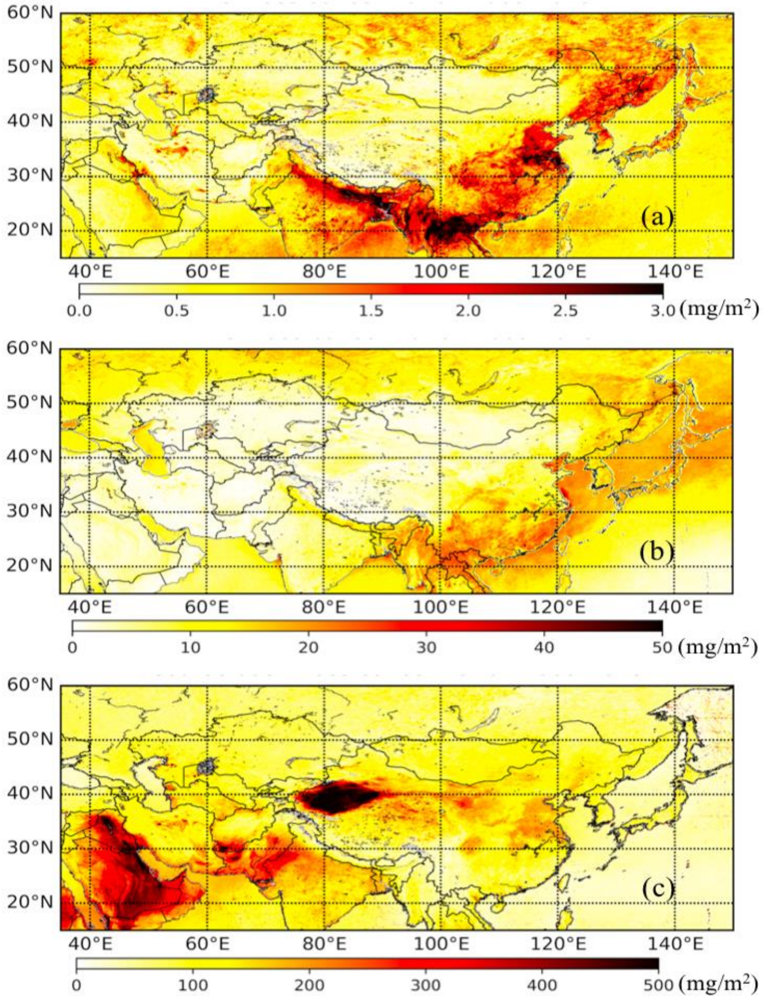

Figure 8: Climatology of aerosol component columnar mass concentration derived from POLDER-3 over East-Asia by the GRASP/Components approach: (a) fine mode black carbon, (b) fine mode brown carbon, (c) coarse mode mineral dust.

While, the validation and analysis of aerosol composition retrieval is very complex and conceptually not evident, qualitative agreement of compositional spatial patterns has been be clearly recognized (e.g., Li et al. 2020a, 2020b). For example, Fig. (9) illustrates impressive qualitative agreement of the BC mass concentration retrieval by POLDER/Components with simulation of GOCART model (Chin et al, 2002). Therefore, taking into consideration both high accuracy of aerosol optical properties provided by "Components approach" and frequent qualitative of retrieved aerosol composition spatial patent with the expectations, this approach can be considered as very promising approach for both future evolution of aerosol remote sensing and the efforts on harmonizing remote sensing approaches with those of CTMs.

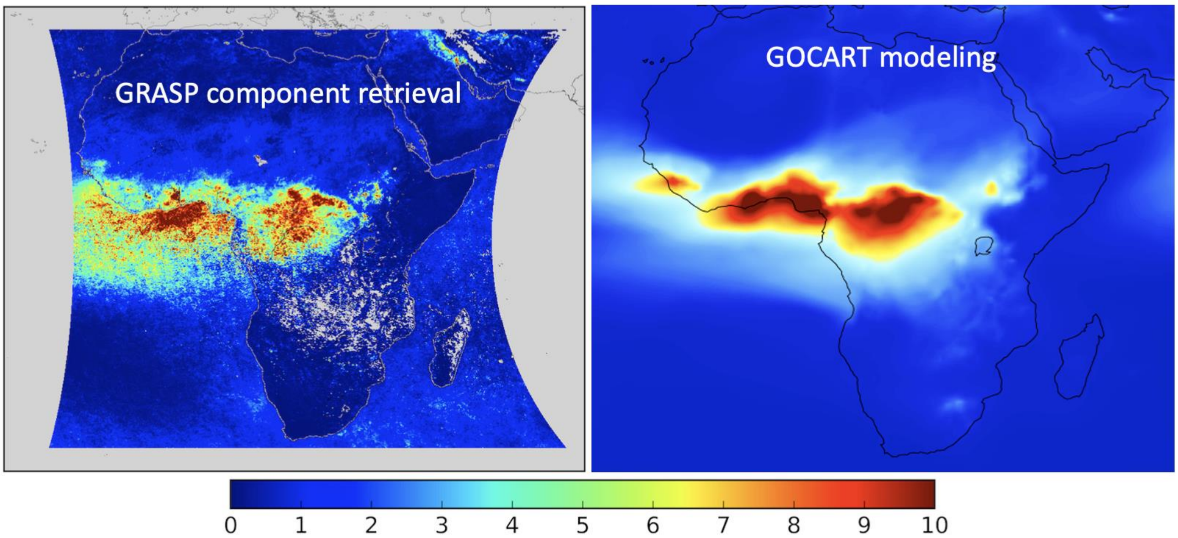

Figure 8: Black Carbon mass concentration(mg/m^2) in January 2008: retrieved by GRASP/Components approach (left), simulated by GOCART model.

Thus, the MAP aerosol products that generated using GRASP/Components approach provides to the user the wealth of information about aerosol. The provided data should give to the potential user an example of the extended aerosol product that is planned to be available from 3MI/EPS-SG products. Specifically, the users can:

(i) analyze the detailed aerosol optical properties including spectral AOD, AODF, AODC, SSA, AAOD, etc. There properties are available from both provided data sets POLDER/Models and POLDER/Components. At the same time, the second data set should provide more accurate and consistent product (as was discussed above).
(ii) analyze, in addition, suggested composition distribution of aerosol: such as black carbon, brown carbon, fine/coarse mode non-absorbing soluble and insoluble, coarse mode absorbing and aerosol water. This additional information is expected to be useful for assimilation and constraining the CTM, specifically CAMS.

Figures 9 and 10 illustrate the above statements. Namely, Figure 9 shows the global maps of 2008 mean AOD, AE, AODF and AODC at 565 nm. As one can see that the maps of AE, AODF and AODC provide rather clear geographical patterns distribution of fine and coarse particle aerosol that should be helpful for diverse user applications. It can be seen that globally coarse AODC and aerosol with low AE are associated with desert dust, while the out brakes of AODF and aerosol with high AE are related with biomass burning events and urban pollution. These maps of the detailed optical characteristics were plotted using second data set (POLDER/Components), while the first data set (POLDER/Models) also include them (whole some of the parameter: AE, AODF and AODC somewhat less accurate).

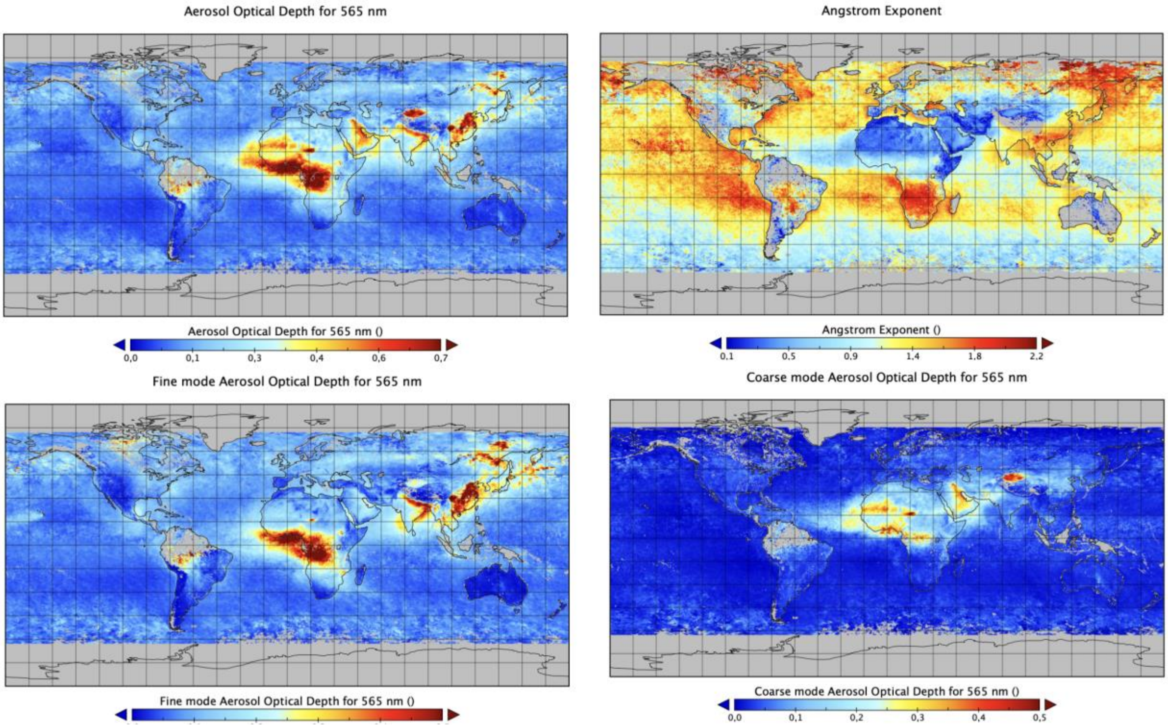

Figure 9: The global maps of 2008 mean AOD AE, AODF and AODC at 565 nm generated as part of Level 3, 0.1 degree resolution POLDER/Component aerosol product.

In a contrast, Figure 10 illustrates the information that available only in the POLDER/Components data set. Figure 10 displays AAOD at 443nm together with mass concentrations of main aerosol fine mode absorbers BC and BrC and Iron Oxide that determines the level of absorption of desert dust. This provide very interesting observation of aerosol absorption origins. It can be clearly seen from the maps that in general BC has strong presence in African biomass burning and also has presence in smoke events over Canada and Russia and urban pollution. According to the maps, the BrC is probably dominant absorber in Canadian and Russia fire smoke and significant presence in urban polluted areas and in African smoke. Certainly, there data are only one of the first data set providing information about aerosol composition from satellite observations and the accuracy and even overall validity of this product needs to be verified and improved in the future.

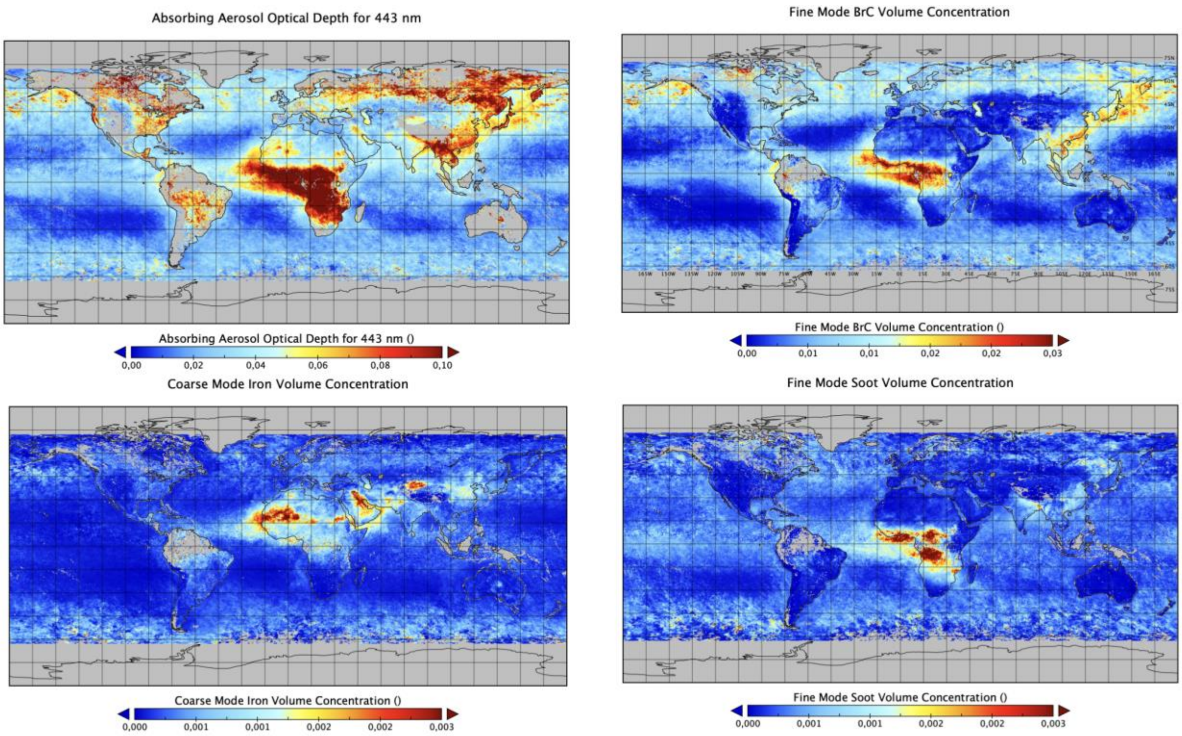

Figure 10: The global maps of 2008 mean AAOD (443), the mass concentrations (kg/m^2) of main aerosol absorbers fine mode BC and BrC and coarse mode Iron Oxide generated as part of Level 3, 0.1 degree resolution POLDER/Component aerosol product.

1.2.3 The advances in retrieval of aerosol composition information from multi-angular polarimetric observation (3MI proxy retrieval)

As already mentioned, the delivered 3MI Proxy POLDER/Components aerosol product (second delivered data set) doesn't represent the latest configuration of aerosol modelling concept developed in CAMEO project. Since the global processing of POLDER data takes significant efforts and computational resource, this delivery includes one of intermediate POLDER/Components version that allow more accurate, compared to initial POLDER products, retrieval of optical properties and provide aerosol retrieval product that has rather harmonious concept with that of CTM and CAMS specifically. At the same time, there are significant effort in frame of CAMEO project on further harmonization of aerosol remote sensing retrievals with CAMS. These efforts are described in details in D1.4 document by Litvinov et al., (2024) and summarized in Table 2.

	Feasibility tests	Performance in AOD	Performance in SSA	Performance in AE
1	Volume mixture	Same quality	Same quality	Same quality
2	SU in separate mode	Decreased	Improved	Decreased
3	Sea Salt and Dust in separates modes	Same quality	Improved	Improved
4	Hydrophobic BC and BrC in the separate modes	Decreased	Improved	Decreased

	Feasibility tests	Performance in AOD	Performance in SSA	Performance in AE
5	Adjustment of the complex refractive index of aerosol chemical components	Same quality	Same quality	Same quality

Table 2. Feasibility tests summary (adapted from Table 5.1 of D1.4, Litvinov et al., 2024)

Once of the overall conclusion of all these tests will be achieved, the global processing of POLDER data can be realized and the aerosol product can be built with the most advanced retrieval configuration. Nonetheless, in order to provide interested user some inside of possible improvement, we added this third data set in as part of delivered data, because that includes the retrieval of the presently the best POLDER/Components configuration (see Table 2) that, in difference with previous version of the Components approach considers Sea Salt and Dust in separates externally mixed modes. The data set provides the data globally over AERONET site (see details in D1.4, Litvinov et al., 2024).

2 Data sets and formats

The delivered data archive includes three data sets:

(1) The first data set includes POLDER-3/GRASP aerosol product generated using POLDER-3/Models (e.g., Chen et al., 2020, Dubovik et al., 2021). This product includes comprehensive set of aerosol optical properties. It also includes parameters of BRDF and BPRDF describing surface reflectance properties. The complete list of parameters is listed the Section 5.1 of the Annex. This is a global data set, for a year 2008.

(2) The second data set includes POLDER-3/GRASP aerosol product generated using POLDER-3/Components (e.g., Lei et al., 2019, Dubovik et al., 2021). This product includes comprehensive set of aerosol optical properties and surface reflectance properties. In addition, this data set includes the parameters charactering aerosol components that, as discussed in D1.4 (Litvinov et al., 2024), provide information in aerosol composition in manner aligned to CTM and especially to CAMS. The complete list of parameters is listed in the Section 5.2 of the Annex. This is a global data set, for a year 2008.

(3) The third data set includes POLDER-3/GRASP aerosol product generated using GRASP/Components with the latest version of aerosol model representation that discussed in D.1.4 (Litvinov, et al., 2024). In difference with second data set, this processing provided two externally mixed aerosol modes: fine mode, coarse desert dust, and coarse sea salt. In This approach, in a contrast with previous retrieve different size distributions for desert dust and sea salt aerosol coarse modes of aerosol. In a contrast to the two first data sets, this data sat is only over AERONET sites, for a year 2008.

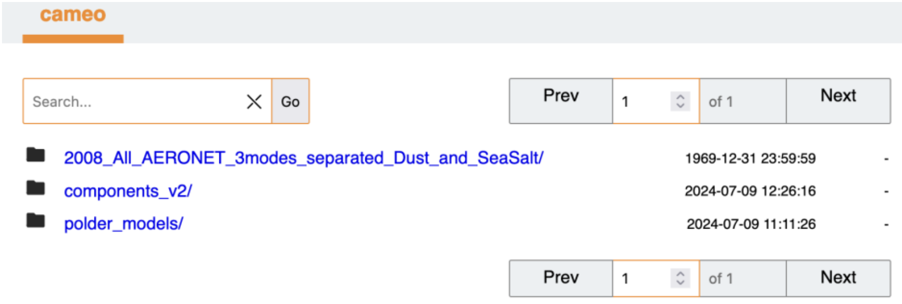

Figure 11: The illustration of delivered data sets at the website.

Download of GRASP products is available via the current Products page:

https://download.grasp-sas.com/download/cameo/

Figure 11 shows the presentation of delivered data sets at the website. There are two options of download:

• Interactively via the website and the normal GRASP Single-Sign-On (click the 'Download' button above).

• Once you try to **"Sign-In" for the first time**, you will be asked to register by providing basic information. Please, register, this takes just a few moments. Once approved by the server security (this is just a formality), the assess will be granted to the data sets.

• Using HTTPS Basic Authentication for downloading data in a batch script (useful for big number of files). Click 'Download' above, the *wget* command appears in the bottom of the webpage. When a new directory is accessed, the *wget* command will be automatically updated to download all the data files that fall under this directory.

2.1 The description of archive organizations

The first and the second data archives have rather comprehensive data organization and representation that is designed for the convenience and in the interest of scientific data user, as illustrated by Fig.(12). The third data set includes only the data provided directly by the GRASP output. No additional optimization of the data set was provided since this archive represents only intermediate test results provided only over AERONET site as illustrated by Fig.(13). Once the new approach will be finalized and the global data set generated the data will be provide in the similar manner as it is done for two first data sets.

The first and the second data archives have the following structure, illustrated by Fig.(12):

Internal archives (not available in the download).
Level 1: GRASP output
Level 1: Internal. Tile output files. Level 1.5 internal: daily and not -filtered

The access to the internal archive could be provided under request. Please, contact us (https://www.grasp-open.com/contact/) for further information.

Public files provided in this deliverable:

Level 2: Data filtered at 6 km resolution, sinusoidal projection

- *daily*
- *monthly*
- *seasonal*
- *yearly*
- *climatological:*
    - *monthly*
    - *seasonal*
    - *yearly*

Level 3 : Regrid level 2

- *0.1 degree :*
    - *daily*
    - *monthly*
    - *seasonal*
    - *yearly*
    - *climatological (averaged over all years of archive)*
        - *monthly*
        - *seasonal*
        - *yearly*

- *1 degree :*
    - *daily*
    - *monthly*
    - *seasonal*
    - *yearly*
    - *climatological:*
        - *monthly*
        - *seasonal*
        - *yearly.*

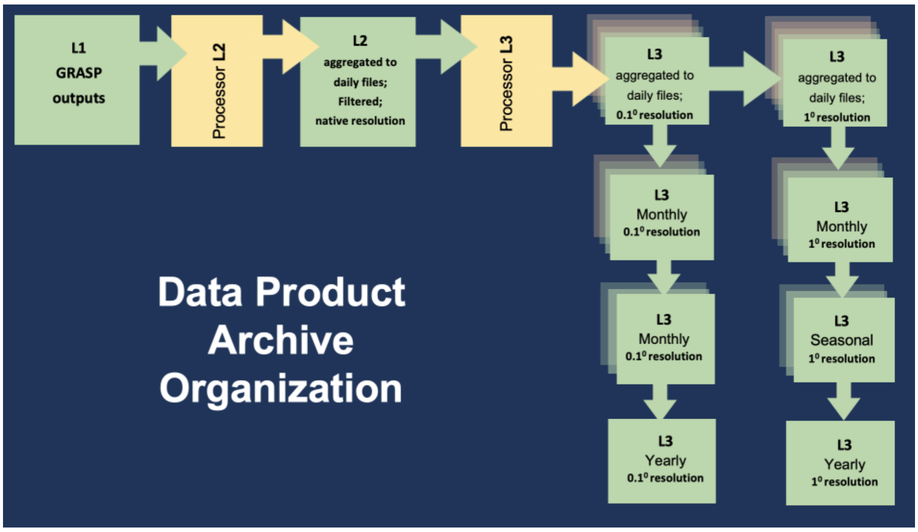

Figure 12: The illustration of the first and second data archive organizations.

cameo > 2008_All_AERONET_3modes_separated_Dust_and_SeaSalt

Search... Go Prev 1 of 24 Next

ATHENS-NOA.parasol_grasp.2008-01-03_2008-03-31.csv	2023-08-21 06:00:30	229.0 KiB
ATHENS-NOA.parasol_grasp.2008-04-07_2008-07-02.csv	2023-08-19 22:02:24	285.1 KiB
ATHENS-NOA.parasol_grasp.2008-07-04_2008-09-30.csv	2023-08-20 01:29:30	493.1 KiB
ATHENS-NOA.parasol_grasp.2008-10-04_2008-12-25.csv	2023-08-18 16:53:39	179.4 KiB
Abu_Al_Bukhoosh.parasol_grasp.2008-01-01_2008-03-31.csv	2023-08-18 16:17:12	468.3 KiB
Abu_Al_Bukhoosh.parasol_grasp.2008-04-02_2008-07-02.csv	2023-08-20 00:35:48	603.6 KiB
Abu_Al_Bukhoosh.parasol_grasp.2008-07-04_2008-10-02.csv	2023-08-19 04:34:13	687.8 KiB
Abu_Al_Bukhoosh.parasol_grasp.2008-10-04_2008-12-30.csv	2023-08-21 01:44:10	471.6 KiB
Agoufou.parasol_grasp.2008-01-04_2008-03-31.csv	2023-08-21 03:50:58	546.5 KiB
Agoufou.parasol_grasp.2008-04-03_2008-06-28.csv	2023-08-19 12:51:53	443.8 KiB
Agoufou.parasol_grasp.2008-07-03_2008-10-02.csv	2023-08-19 13:59:17	378.0 KiB
Agoufou.parasol_grasp.2008-10-04_2008-12-28.csv	2023-08-18 15:38:09	601.1 KiB
Alta_Floresta.parasol_grasp.2008-01-03_2008-03-09.csv	2023-08-18 17:19:45	27.7 KiB
Alta_Floresta.parasol_grasp.2008-06-06_2008-06-27.csv	2023-08-19 20:52:23	82.2 KiB
Alta_Floresta.parasol_grasp.2008-07-15_2008-09-24.csv	2023-08-20 12:42:47	237.5 KiB
Alta_Floresta.parasol_grasp.2008-10-05_2008-12-09.csv	2023-08-18 20:30:59	45.9 KiB
Ames.parasol_grasp.2008-03-10_2008-03-25.csv	2023-08-20 01:07:56	60.7 KiB
Ames.parasol_grasp.2008-04-04_2008-07-01.csv	2023-08-18 20:21:40	316.8 KiB
Ames.parasol_grasp.2008-07-10_2008-09-29.csv	2023-08-18 22:35:45	318.5 KiB
Ames.parasol_grasp.2008-10-03_2008-12-29.csv	2023-08-20 13:20:30	260.5 KiB
Amsterdam_Island.parasol_grasp.2008-01-01_2008-04-01.csv	2023-08-20 07:37:50	298.7 KiB
Amsterdam_Island.parasol_grasp.2008-04-03_2008-07-01.csv	2023-08-20 02:35:39	168.2 KiB
Amsterdam_Island.parasol_grasp.2008-07-03_2008-10-01.csv	2023-08-19 22:30:23	255.7 KiB
Amsterdam_Island.parasol_grasp.2008-10-03_2008-12-29.csv	2023-08-20 17:54:25	274.0 KiB
Andenes.parasol_grasp.2008-03-18_2008-03-30.csv	2023-08-19 08:12:44	80.5 KiB
Andenes.parasol_grasp.2008-04-02_2008-06-30.csv	2023-08-19 00:01:01	524.5 KiB
Andenes.parasol_grasp.2008-07-04_2008-09-23.csv	2023-08-18 10:48:52	402.4 KiB
Appledore_Island.parasol_grasp.2008-01-03_2008-03-30.csv	2023-08-18 19:22:50	402.6 KiB
Appledore_Island.parasol_grasp.2008-04-03_2008-07-01.csv	2023-08-19 15:35:03	410.9 KiB
Appledore_Island.parasol_grasp.2008-07-04_2008-09-27.csv	2023-08-18 19:46:08	462.1 KiB
Appledore_Island.parasol_grasp.2008-10-03_2008-12-29.csv	2023-08-19 08:51:47	412.6 KiB
Arcachon.parasol_grasp.2008-01-04_2008-03-31.csv	2023-08-19 05:25:02	230.6 KiB
Arcachon.parasol_grasp.2008-04-04_2008-06-30.csv	2023-08-21 04:08:25	285.1 KiB
Arcachon.parasol_grasp.2008-07-04_2008-09-29.csv	2023-08-18 12:50:23	314.9 KiB
Arcachon.parasol_grasp.2008-10-03_2008-12-22.csv	2023-08-20 01:41:03	136.6 KiB
Arica.parasol_grasp.2008-01-02_2008-03-31.csv	2023-08-19 14:25:23	436.1 KiB
Arica.parasol_grasp.2008-04-03_2008-07-01.csv	2023-08-18 11:21:36	464.2 KiB
Arica.parasol_grasp.2008-07-03_2008-10-02.csv	2023-08-20 08:58:52	459.2 KiB
Arica.parasol_grasp.2008-10-03_2008-12-28.csv	2023-08-20 08:11:29	396.4 KiB
Ascension_Island.parasol_grasp.2008-01-01_2008-03-31.csv	2023-08-18 09:59:52	338.2 KiB

Prev 1 of 24 Next

Figure 13: The illustration of the third data archive organizations=.

2.2 The post-processing and data aggregation.

The raw results files from GRASP contain three months of data of small regions (162×162 pixels). For the convenience of the users, the daily global files were created as well as their aggregates in time and space. Only the most reliable and demanded data were exported for final public distribution. Data format of this public archives is NetCDF.

In order to assure higher quality of the data, some post-processing was applied in order to eliminate the low quality points resulted from cloud contamination, bad surface description near the coast, etc. It should be noted that the files include all parameters produced by retrieval, i.e. retrieved surface reflectance parameters are also included.

The post-processing screening follows these steps:

- First, from raw GRASP output we create global daily **level 1** files.
- Pixels with AOD443 > 10 are removed.
- The coast is removed so all pixels with land percent between 1 and 99 are removed. Also, to guarantee a proper coast elimination, the first pixel into ocean and land is removed.
- We remove unphysical values like water surface model over land and the other way around.
- We apply a criteria over to screen bad pixels (retrieval error is high so we remove completely the pixel):
    - ocean → (residual <= 0.13) # In case of “models” archive the threshold for residual is 0.3
    - land :
        - If precondition **ndvi < 0.1**
            - if (dhr670 >= 0.3) then
                - if (AOD670<1) then (residual <= 0.04) # In case of “models” archive the threshold for residual is 0.06
                - else (residual <= 0.06) # In case of “models” archive the threshold for residual is 0.08
            - (dhr670 < 0.3) -> (residual <= 0.07) # In case of “models” archive the threshold for residual is 0.09
        - precondition **0.1 <= ndvi < 0.4**
            - (dhr670 >= 0.25) -> (residual <= 0.075) # In case of “models” archive the threshold for residual is 0.095
            - (dhr670 < 0.25) -> (residual <= 0.085) # In case of “models” archive the threshold for residual is 0.105
        - precondition **0.4 <= ndvi < 0.6**
            - (residual <= 0.1) # In case of “models” archive the threshold for residual is 0.12
        - precondition **0.6 <= ndvi < 1**
            - (residual <= 0.12) # In case of “models” archive the threshold for residual is 0.14
- Extra filter applied only to “models” archive: If any DHR value is missing or DHR(443) < 0, we remove entire pixel (usually snow contamination)
- The «components» archive is postprocessed using the same filtering criteria as for the «models» archive

The date passed all above filter files are stored under **level 1.5**. These data are not publicly available, but can be provided by a special request. This archive ensures good surface retrieval but quality of aerosol products is not guaranteed.

Then,

- the outliers are screened analyzing groups of 20×20 pixels and iteratively we remove the worst pixel (farther to the mean of AOD870) if the group does not fulfil the following condition “std of data <= 1.5 AND std / mean of data <= 0.5”. If the result group has less than 60 pixels it is completely removed (noisy area probably due to cloud contamination).
- Some aerosol products can only be calculated when there is some aerosol loading (otherwise it is difficult to measure them). So, we apply extra filters. Angstrom Exponent is only provided if AOD560 is higher than 0.02 over ocean or 0.2 over land.

Other more complex products (SSA, Re(m), Im(m), AAOD, Size distribution, SphereFraction) are strongly filtered:
  - land : AOD443 >= 0.3 and 0.65 <= SSA <= 1.
  - ocean : AOD443 >= 0.02 and 0.65 <= SSA <= 1.
- These results are exported as **level 2**. Level 2 is also temporally aggregated. The temporal aggregation pixels are removed if AOD443>4.

Level 3 is created as regridding products at 0.1 and 1 degrees resolution in WGS84 projection of data available in level 2. In the regridding process we applied median filter instead of average or any other sophisticated filter.

SSA For aggregation to 1 degree, the following strategy was used for the SSA: SSA(1 degree, Level 3)=Sum(SSA(0.1 degree Level 2)*TAU(0.1 degree Level 2)/(SumTAU(0.1 degree Level 2)

AAOD (1 degree, level 3) = Sum(AAOD(0.1 degree Level 2))/N, where N is a number of 0.1 degree Level 2 pixels used in the Sum.

- In summary, the following data sets are prepared:
  Level 0: raw results from grasp
  Level 1: daily files from the output
  Level 1.5: data softly screened. All surface pixels are good but we cannot guarantee the quality of aerosol information
  Level 2: Full resolution data filtered and aggregations (daily, monthly, yearly, seasonal, and climatologically monthly, seasonal and full archive).
  Level 3: Regirded at 0.1 and 1 degree of level 2 (including temporal aggregations).

3 Summary

Thus, the purpose of this report is to introduce and describe the delivered 3MI Proxy aerosol retrieval data sets. The delivered product archive included the three data sets:

- A set of conventional aerosol optical product of 3MI Proxy observations (GRASP/Models);
- A set of advanced aerosol optical product of 3MI Proxy observations (GRASP/Components). This aerosol data set is an example of aerosol remote sensing aligned with aerosol assumptions used in chemical transport models (CTM);
- A set of improved advanced aerosol optical product of 3MI Proxy observations (GRASP/Components). This improved aerosol illustrative data set that generated using the latest development within CAMEO aimed to improve aligning of remote sensing products with chemical transport models (CTM) and CAMS specifically.

The report outlines the advantages of new extensive advanced aerosol products expected from MAP. It also discusses the potential of the aerosol products generated using remote sensing retrievals aligned with chemical transport models (CTM) and CAMS specifically. The report describes the organization of the provided data archives, the principles of their generation.

4 References

Chen, C., O. Dubovik, D. Fuertes, P. Litvinov, T. Lapyonok, A. Lopatin, F. Ducos, Y. Derimian, M. Herman, D. Tanré, L. A. Remer, A. Lyapustin, A. M. Sayer, R. C. Levy, C. Hsu, J. Descloitres, L. Li, B. Torres, Y. Karol, M. Herrera, M. Herreras, M. Aspetsberger, M. Wanzenboeck, L. Bindreiter, D. Marth, A. Hangler, and C. Federspiel, Validation of GRASP algorithm product from POLDER/PARASOL data and assessment of multi-angular polarimetry potential for aerosol monitoring, Earth System Science Data, 12, 3573–3620, https://doi.org/10.5194/essd-12-3573-2020, 2020.

Chin M., Ginoux P., Kinne S., Torres O., Holben B., Duncan B., Martin R., Logan J., Higurashi A., and Nakajima T. Tropospheric Aerosol Optical Thickness from the GOCART Model and Comparisons with Satellite and Sun Photometer Measurements. J. Atm. Sci., 59, 2002

Dubovik, O., & King, M. D. (2000). A flexible inversion algorithm for retrieval of aerosol optical properties from Sun and sky radiance measurements. Journal of Geophysical Research: Atmospheres, 105(D16), 20673–20696. https://doi.org/10.1029/2000JD900282

Dubovik, O. et al.: Accuracy assessments of aerosol optical properties retrieved from Aerosol Robotic Network (AERONET) Sun and sky radiance measurements, J. Geophys. Res., 105, 9791–9806, https://doi.org/10.1029/2000JD900040, 2000.

Dubovik, O. et al.: Application of spheroid models to account for aerosol particle nonsphericity in remote sensing of desert dust, J. Geophys. Res.-Atmos., 111, D11208, https://doi.org/10.1029/2005JD006619, 2006.

Dubovik, O. et al.: Statistically optimized inversion algorithm for enhanced retrieval of aerosol properties from spectral multi-angle polarimetric satellite observations, Atmos. Meas. Tech., 4, 975–1018, https://doi.org/10.5194/amt-4-975-2011, 2011.

Dubovik, O. et al.: GRASP: a versatile algorithm for characterizing the atmosphere, SPIE: Newsroom, https://doi.org/10.1117/2.1201408.005558, 2014.

Dubovik, O. et al.: Synergy of PARASOL and CALIOP observations using GRASP algorithm for enhanced aerosol characterisation. In AGU Fall Meeting Abstracts (Vol. 2019, pp. A23B-05), 2019.

Dubovik, O. et al.: A comprehensive description of multi-term LSM for applying multiple a priori constraints in problems of atmospheric remote sensing: GRASP algorithm, concept, and applications, Front. Remote Sens., 2, 23, https://doi.org/10.3389/frsen.2021.706851, 2021.

Hasekamp, O. P. et al.: Aerosol properties over the ocean from PARASOL multiangle photopolarimetric measurements, J. Geophys. Res. Atmos., 116, D14204, https://doi.org/10.1029/2010JD015469, 2011.

Hasekamp, O., P. Litvinov, G., Fu, C., Chen, and O. Dubovik,: Algorithm evaluation for polar-imetric remote sensing of atmospheric aerosols, Atmos. Meas. Tech., 17, 1497–1525, 2024. https://doi.org/10.5194/amt-17-1497-2024.

Fu, G. and Hasekamp, O.: Retrieval of aerosol microphysical and optical properties over land using a multimode approach, Atmos. Meas. Tech., 11, 6627-6650, https://doi.org/10.5194/amt-11-6627-2018, 2018.

Li., L., O. Dubovik, Y. Derimian, G. L. Schuster, T. Lapyonok, P. Litvinov, F. Ducos, D. Fuertes, C. Chen, Z. Li, A. Lopatin, B. Torres and H. Che, “Retrieval of aerosol components directly from satellite and ground-based measurements”, Atmos. Chem. Phys. 19, 13409–13443, https://doi.org/10.5194/acp-19-13409-2019, 2019.

Li, J. et al.: Synergy of satellite- and ground-based aerosol optical depth measurements using an ensemble Kalman filter approach, J. Geophys. Res. Atmos., 125, e2019JD031884, 2020. https://doi.org/10.1029/2019JD031884, 2020a.

Li, L. et al.: Retrievals of fine mode light-absorbing carbonaceous aerosols from POLDER/PARASOL observations over East and South Asia, Remote Sens. Environ., 247, 111913, 2020. https://doi.org/10.1016/j.rse.2020.111913, 2020b.

Litvinov, P., O. Dubovik, C. Chen, M. Herrera, C. Matar, M. Herreras, and A. Lopatin, CAMEO, D1.4: “Report on aligning aerosol parameter retrievals”, 2024.

Zhang, X. et al.: Validation of the aerosol optical property products derived by the GRASP/Component approach from multi-angular polarimetric observations, Atmos. Res., 263, 105802,https://doi.org/10.1016/j.atmosres.2021.105802, 2021.

Document History

Version	Author(s)	Date	Changes
0.1	Oleg Dubovik, Pavel Litvinov, Milagros Herrera, Christian Matar, Marcos Herreras, Anton Lopatin	30/6/2024	Initial version
1.0	Oleg Dubovik, Pavel Litvinov, Milagros Herrera, Christian Matar, Marcos Herreras, Anton Lopatin	12/8/2024	Version 1 released after internal review
1.1	Oleg Dubovik	12/8/2024	Minor correction

Internal Review History

Internal Reviewers	Date	Comments
Johannes Flemming (ECMWF) and Yana Karol (GRASP)	July 2024	Minor comments

5 ANNEX

5.1 ANNEX-1: The list of the parameters provided in POLDER-3 GRASP/Models archive.

Parameter	Data Field in L1	Long Name
datetime	Datetime	Unix Time in seconds counted from 00h.00min00sec 01.01.1970
residual_relative_noise0	ResidualRelative_0	Relative Residual
residual_relative_noise1	ResidualRelative_1	
land_percent	LandPercentage	Percentage of Land
cloud_mask	CloudMask	
SizeDistrLogNormBin1_1	SizeDistrLogNormBin1_1	Aerosol model fraction (smoke)
SizeDistrLogNormBin2_1	SizeDistrLogNormBin2_1	Aerosol model fraction (urban)
SizeDistrLogNormBin3_1	SizeDistrLogNormBin3_1	Aerosol model fraction (oceanic)
SizeDistrLogNormBin1_2	SizeDistrLogNormBin1_2	Aerosol model fraction (dust)
SizeDistrLogNormBin2_2	SizeDistrLogNormBin2_2	Aerosol model fraction (urban polluted)
ndvi	NDVI	Normalized Difference Vegetation Index
SphereFraction	SphereFraction	Sphere Fraction
VertProfileHeight	VertProfileHeight	Mean height of Vertical profile
LandBRDFRossLi443_1	Ross_Li_BRDF_443_isotropic_parameter	Ross Li BRDF isotropic parameter at 443 nm
LandBRDFRossLi490_1	Ross_Li_BRDF_490_isotropic_parameter	Ross Li BRDF isotropic parameter at 490 nm
LandBRDFRossLi565_1	Ross_Li_BRDF_565_isotropic_parameter	Ross Li BRDF isotropic parameter at 565 nm
LandBRDFRossLi670_1	Ross_Li_BRDF_670_isotropic_parameter	Ross Li BRDF isotropic parameter at 670 nm
LandBRDFRossLi865_1	Ross_Li_BRDF_865_isotropic_parameter	Ross Li BRDF isotropic parameter at 865 nm
LandBRDFRossLi1020_1	Ross_Li_BRDF_1020_isotropic_parameter	Ross Li BRDF isotropic parameter at 1020 nm
LandBRDFRossLi443_2	Ross_Li_BRDF_443_volumetric_parameter	Ross Li BRDF normalised volumetric parameter
LandBRDFRossLi490_2	Ross_Li_BRDF_490_volumetric_parameter	Ross Li BRDF normalised volumetric parameter
LandBRDFRossLi565_2	Ross_Li_BRDF_565_volumetric_parameter	Ross Li BRDF normalised volumetric parameter
LandBRDFRossLi670_2	Ross_Li_BRDF_670_volumetric_parameter	Ross Li BRDF normalised volumetric parameter
LandBRDFRossLi865_2	Ross_Li_BRDF_865_volumetric_parameter	Ross Li BRDF normalised volumetric parameter
LandBRDFRossLi1020_2	Ross_Li_BRDF_1020_volumetric_parameter	Ross Li BRDF normalised volumetric parameter
LandBRDFRossLi443_3	Ross_Li_BRDF_443_geometric_parameter	Ross Li BRDF normalised geometric parameter
LandBRDFRossLi490_3	Ross_Li_BRDF_490_geometric_parameter	Ross Li BRDF normalised geometric parameter
LandBRDFRossLi565_3	Ross_Li_BRDF_565_geometric_parameter	Ross Li BRDF normalised geometric parameter
LandBRDFRossLi670_3	Ross_Li_BRDF_670_geometric_parameter	Ross Li BRDF normalised geometric parameter
LandBRDFRossLi865_3	Ross_Li_BRDF_865_geometric_parameter	Ross Li BRDF normalised geometric parameter

LandBRDFRossLi1020_3	Ross_Li_BRDF_1020_geometric_parameter	Ross Li BRDF normalised geometric parameter
LandBPDFMaignanBreon443	LandBPDFMaignanBreon443	
LandBPDFMaignanBreon490	LandBPDFMaignanBreon490	
LandBPDFMaignanBreon565	LandBPDFMaignanBreon565	
LandBPDFMaignanBreon670	LandBPDFMaignanBreon670	
LandBPDFMaignanBreon865	LandBPDFMaignanBreon865	
LandBPDFMaignanBreon1020	LandBPDFMaignanBreon1020	
WaterBRMCoxMunkIso443_1	Cox_Munk_iso_BRM_443_first_parameter	Surface albedo of water body at 443 nm
WaterBRMCoxMunkIso490_1	Cox_Munk_iso_BRM_490_first_parameter	Surface albedo of water body at 490 nm
WaterBRMCoxMunkIso565_1	Cox_Munk_iso_BRM_565_first_parameter	Surface albedo of water body at 565 nm
WaterBRMCoxMunkIso670_1	Cox_Munk_iso_BRM_670_first_parameter	Surface albedo of water body at 670 nm
WaterBRMCoxMunkIso865_1	Cox_Munk_iso_BRM_865_first_parameter	Surface albedo of water body at 865 nm
WaterBRMCoxMunkIso1020_1	Cox_Munk_iso_BRM_1020_first_parameter	Surface albedo of water body at 1020 nm
WaterBRMCoxMunkIso443_2	Cox_Munk_iso_BRM_443_second_parameter	Fraction of Fresnel reflection contribution at 443nm
WaterBRMCoxMunkIso490_2	Cox_Munk_iso_BRM_490_second_parameter	Fraction of Fresnel reflection contribution at 490nm
WaterBRMCoxMunkIso565_2	Cox_Munk_iso_BRM_565_second_parameter	Fraction of Fresnel reflection contribution at 565nm
WaterBRMCoxMunkIso670_2	Cox_Munk_iso_BRM_670_second_parameter	Fraction of Fresnel reflection contribution at 670nm
WaterBRMCoxMunkIso865_2	Cox_Munk_iso_BRM_865_second_parameter	Fraction of Fresnel reflection contribution at 865nm
WaterBRMCoxMunkIso1020_2	Cox_Munk_iso_BRM_1020_second_parameter	Fraction of Fresnel reflection contribution at 1020nm
WaterBRMCoxMunkIso443_3	Cox_Munk_iso_BRM_443_third_parameter	Mean square ocean surface slope at 443 nm
WaterBRMCoxMunkIso490_3	Cox_Munk_iso_BRM_490_third_parameter	Mean square ocean surface slope at 490 nm
WaterBRMCoxMunkIso565_3	Cox_Munk_iso_BRM_565_third_parameter	Mean square ocean surface slope at 565 nm
WaterBRMCoxMunkIso670_3	Cox_Munk_iso_BRM_670_third_parameter	Mean square ocean surface slope at 670 nm
WaterBRMCoxMunkIso865_3	Cox_Munk_iso_BRM_865_third_parameter	Mean square ocean surface slope at 865 nm
WaterBRMCoxMunkIso1020_3	Cox_Munk_iso_BRM_1020_third_parameter	Mean square ocean surface slope at 1020 nm
AExp	AExp	Angstrom Exponent (665nm-865nm)
tau443	AOD443	Aerosol Optical Depth for 443 nm
tau490	AOD490	Aerosol Optical Depth for 490 nm
tau565	AOD565	Aerosol Optical Depth for 565 nm
tau670	AOD670	Aerosol Optical Depth for 670 nm
tau865	AOD865	Aerosol Optical Depth for 865 nm
tau1020	AOD1020	Aerosol Optical Depth for 1020 nm

aaod443	AAOD443	Absorbing Aerosol Optical Depth for 443 nm
aaod490	AAOD490	Absorbing Aerosol Optical Depth for 490 nm
aaod565	AAOD565	Absorbing Aerosol Optical Depth for 565 nm
aaod670	AAOD670	Absorbing Aerosol Optical Depth for 670 nm
aaod865	AAOD865	Absorbing Aerosol Optical Depth for 865 nm
aaod1020	AAOD1020	Absorbing Aerosol Optical Depth for 1020 nm
tau443_0	AODF443	Fine mode AOD at 443 nm
tau443_1	AODC443	Coarse mode AOD at 443 nm
tau490_0	AODF490	Fine mode AOD at 490 nm
tau490_1	AODC490	Coarse mode AOD at 490 nm
tau565_0	AODF565	Fine mode AOD at 565 nm
tau565_1	AODC565	Coarse mode AOD at 565 nm
tau670_0	AODF670	Fine mode AOD at 670 nm
tau670_1	AODC670	Coarse mode AOD at 670 nm
tau865_0	AODF865	Fine mode AOD at 865 nm
tau865_1	AODC865	Coarse mode AOD at 865 nm
tau1020_0	AODF1020	Fine mode AOD at 1020 nm
tau1020_1	AODC1020	Coarse mode AOD at 1020 nm
ssa443	SSA443	Single Scattering Albedo at 443 nm
ssa490	SSA490	Single Scattering Albedo at 490 nm
ssa565	SSA565	Single Scattering Albedo at 565 nm
ssa670	SSA670	Single Scattering Albedo at 670 nm
ssa865	SSA865	Single Scattering Albedo at 865 nm
ssa1020	SSA1020	Single Scattering Albedo at 1020 nm
salbedo443	DHR443	Directional Hemispherical Reflectance at 443 nm
salbedo490	DHR490	Directional Hemispherical Reflectance at 490 nm
salbedo565	DHR565	Directional Hemispherical Reflectance at 565 nm
salbedo670	DHR670	Directional Hemispherical Reflectance at 670 nm
salbedo865	DHR865	Directional Hemispherical Reflectance at 865 nm
salbedo1020	DHR1020	Directional Hemispherical Reflectance at 1020 nm

Table 3: POLDER-3 GRASP/Models product specification.

5.2 ANNEX-2: The list of the parameters provided in POLDER-3 GRASP/Components archive.

Parameter	Data Field in L1	Long Name
datetime	Datetime	Unix Time in seconds counted from 00h.00min00sec 01.01.1970
residual_relative_noise0	ResidualRelative_0	Relative Residual
residual_relative_noise1	ResidualRelative_1	
land_percent	LandPercentage	Percentage of Land
cloud_mask	CloudMask	
SizeDistrLogNormBin1_1	SizeDistrLogNormBin1_1	
SizeDistrLogNormBin2_1	SizeDistrLogNormBin2_1	
SizeDistrLogNormBin3_1	SizeDistrLogNormBin3_1	
SizeDistrLogNormBin1_2	SizeDistrLogNormBin1_2	
SizeDistrLogNormBin2_2	SizeDistrLogNormBin2_2	
ndvi	NDVI	Normalized Difference Vegetation Index
SphereFraction	SphereFraction	Sphere Fraction
VertProfileHeight	VertProfileHeight	Mean height of Vertical profile
LandBRDFRossLi443_1	Ross_Li_BRDF_443_isotropic_parameter	Ross Li BRDF isotropic parameter at 443 nm
LandBRDFRossLi490_1	Ross_Li_BRDF_490_isotropic_parameter	Ross Li BRDF isotropic parameter at 490 nm
LandBRDFRossLi565_1	Ross_Li_BRDF_565_isotropic_parameter	Ross Li BRDF isotropic parameter at 565 nm
LandBRDFRossLi670_1	Ross_Li_BRDF_670_isotropic_parameter	Ross Li BRDF isotropic parameter at 670 nm
LandBRDFRossLi865_1	Ross_Li_BRDF_865_isotropic_parameter	Ross Li BRDF isotropic parameter at 865 nm
LandBRDFRossLi1020_1	Ross_Li_BRDF_1020_isotropic_parameter	Ross Li BRDF isotropic parameter at 1020 nm
LandBRDFRossLi443_2	Ross_Li_BRDF_443_volumetric_parameter	Ross Li BRDF normalised volumetric parameter
LandBRDFRossLi490_2	Ross_Li_BRDF_490_volumetric_parameter	Ross Li BRDF normalised volumetric parameter
LandBRDFRossLi565_2	Ross_Li_BRDF_565_volumetric_parameter	Ross Li BRDF normalised volumetric parameter
LandBRDFRossLi670_2	Ross_Li_BRDF_670_volumetric_parameter	Ross Li BRDF normalised volumetric parameter
LandBRDFRossLi865_2	Ross_Li_BRDF_865_volumetric_parameter	Ross Li BRDF normalised volumetric parameter
LandBRDFRossLi1020_2	Ross_Li_BRDF_1020_volumetric_parameter	Ross Li BRDF normalised volumetric parameter
LandBRDFRossLi443_3	Ross_Li_BRDF_443_geometric_parameter	Ross Li BRDF normalised geometric parameter
LandBRDFRossLi490_3	Ross_Li_BRDF_490_geometric_parameter	Ross Li BRDF normalised geometric parameter
LandBRDFRossLi565_3	Ross_Li_BRDF_565_geometric_parameter	Ross Li BRDF normalised geometric parameter
LandBRDFRossLi670_3	Ross_Li_BRDF_670_geometric_parameter	Ross Li BRDF normalised geometric parameter
LandBRDFRossLi865_3	Ross_Li_BRDF_865_geometric_parameter	Ross Li BRDF normalised geometric parameter
LandBRDFRossLi1020_3	Ross_Li_BRDF_1020_geometric_parameter	Ross Li BRDF normalised geometric parameter

LandBPDFMaignanBreon443	LandBPDFMaignanBreon443	
LandBPDFMaignanBreon490	LandBPDFMaignanBreon490	
LandBPDFMaignanBreon565	LandBPDFMaignanBreon565	
LandBPDFMaignanBreon670	LandBPDFMaignanBreon670	
LandBPDFMaignanBreon865	LandBPDFMaignanBreon865	
LandBPDFMaignanBreon1020	LandBPDFMaignanBreon1020	
WaterBRMCoxMunkIso443_1	Cox_Munk_iso_BRM_443_first_parameter	Surface albedo of water body at 443 nm
WaterBRMCoxMunkIso490_1	Cox_Munk_iso_BRM_490_first_parameter	Surface albedo of water body at 490 nm
WaterBRMCoxMunkIso565_1	Cox_Munk_iso_BRM_565_first_parameter	Surface albedo of water body at 565 nm
WaterBRMCoxMunkIso670_1	Cox_Munk_iso_BRM_670_first_parameter	Surface albedo of water body at 670 nm
WaterBRMCoxMunkIso865_1	Cox_Munk_iso_BRM_865_first_parameter	Surface albedo of water body at 865 nm
WaterBRMCoxMunkIso1020_1	Cox_Munk_iso_BRM_1020_first_parameter	Surface albedo of water body at 1020 nm
WaterBRMCoxMunkIso443_2	Cox_Munk_iso_BRM_443_second_parameter	Fraction of Fresnel reflection contribution at 443nm
WaterBRMCoxMunkIso490_2	Cox_Munk_iso_BRM_490_second_parameter	Fraction of Fresnel reflection contribution at 490nm
WaterBRMCoxMunkIso565_2	Cox_Munk_iso_BRM_565_second_parameter	Fraction of Fresnel reflection contribution at 565nm
WaterBRMCoxMunkIso670_2	Cox_Munk_iso_BRM_670_second_parameter	Fraction of Fresnel reflection contribution at 670nm
WaterBRMCoxMunkIso865_2	Cox_Munk_iso_BRM_865_second_parameter	Fraction of Fresnel reflection contribution at 865nm
WaterBRMCoxMunkIso1020_2	Cox_Munk_iso_BRM_1020_second_parameter	Fraction of Fresnel reflection contribution at 1020nm
WaterBRMCoxMunkIso443_3	Cox_Munk_iso_BRM_443_third_parameter	Mean square ocean surface slope at 443 nm
WaterBRMCoxMunkIso490_3	Cox_Munk_iso_BRM_490_third_parameter	Mean square ocean surface slope at 490 nm
WaterBRMCoxMunkIso565_3	Cox_Munk_iso_BRM_565_third_parameter	Mean square ocean surface slope at 565 nm
WaterBRMCoxMunkIso670_3	Cox_Munk_iso_BRM_670_third_parameter	Mean square ocean surface slope at 670 nm
WaterBRMCoxMunkIso865_3	Cox_Munk_iso_BRM_865_third_parameter	Mean square ocean surface slope at 865 nm
WaterBRMCoxMunkIso1020_3	Cox_Munk_iso_BRM_1020_third_parameter	Mean square ocean surface slope at 1020 nm
reff_index_real443_0	RealRefIndF443	Fine mode RealRefInd at 443 nm
reff_index_real443_1	RealRefIndC443	Coarse mode RealRefInd at 443 nm
reff_index_real490_0	RealRefIndF490	Fine mode RealRefInd at 490 nm
reff_index_real490_1	RealRefIndC490	Coarse mode RealRefInd at 490 nm
reff_index_real565_0	RealRefIndF565	Fine mode RealRefInd at 565 nm

reff_index_real565_1	RealRefIndC565	Coarse mode RealRefInd at 565 nm
reff_index_real670_0	RealRefIndF670	Fine mode RealRefInd at 670 nm
reff_index_real670_1	RealRefIndC670	Coarse mode RealRefInd at 670 nm
reff_index_real865_0	RealRefIndF865	Fine mode RealRefInd at 865 nm
reff_index_real865_1	RealRefIndC865	Coarse mode RealRefInd at 865 nm
reff_index_real1020_0	RealRefIndF1020	Fine mode RealRefInd at 1020 nm
reff_index_real1020_1	RealRefIndC1020	Coarse mode RealRefInd at 1020 nm
reff_index_imag443_0	ImagRefIndF443	Fine mode ImagRefInd at 443 nm
reff_index_imag443_1	ImagRefIndC443	Coarse mode ImagRefInd at 443 nm
reff_index_imag490_0	ImagRefIndF490	Fine mode ImagRefInd at 490 nm
reff_index_imag490_1	ImagRefIndC490	Coarse mode ImagRefInd at 490 nm
reff_index_imag565_0	ImagRefIndF565	Fine mode ImagRefInd at 565 nm
reff_index_imag565_1	ImagRefIndC565	Coarse mode ImagRefInd at 565 nm
reff_index_imag670_0	ImagRefIndF670	Fine mode ImagRefInd at 670 nm
reff_index_imag670_1	ImagRefIndC670	Coarse mode ImagRefInd at 670 nm
reff_index_imag865_0	ImagRefIndF865	Fine mode ImagRefInd at 865 nm
reff_index_imag865_1	ImagRefIndC865	Coarse mode ImagRefInd at 865 nm
reff_index_imag1020_0	ImagRefIndF1020	Fine mode ImagRefInd at 1020 nm
reff_index_imag1020_1	ImagRefIndC1020	Coarse mode ImagRefInd at 1020 nm
AExp	AExp	Angstrom Exponent (665nm-865nm)
tau443	AOD443	Aerosol Optical Depth for 443 nm
tau490	AOD490	Aerosol Optical Depth for 490 nm
tau565	AOD565	Aerosol Optical Depth for 565 nm
tau670	AOD670	Aerosol Optical Depth for 670 nm
tau865	AOD865	Aerosol Optical Depth for 865 nm
tau1020	AOD1020	Aerosol Optical Depth for 1020 nm
aaod443	AAOD443	Absorbing Aerosol Optical Depth for 443 nm
aaod490	AAOD490	Absorbing Aerosol Optical Depth for 490 nm
aaod565	AAOD565	Absorbing Aerosol Optical Depth for 565 nm

aaod670	AAOD670	Absorbing Aerosol Optical Depth for 670 nm
aaod865	AAOD865	Absorbing Aerosol Optical Depth for 865 nm
aaod1020	AAOD1020	Absorbing Aerosol Optical Depth for 1020 nm
tau443_0	AODF443	Fine mode AOD at 443 nm
tau443_1	AODC443	Coarse mode AOD at 443 nm
tau490_0	AODF490	Fine mode AOD at 490 nm
tau490_1	AODC490	Coarse mode AOD at 490 nm
tau565_0	AODF565	Fine mode AOD at 565 nm
tau565_1	AODC565	Coarse mode AOD at 565 nm
tau670_0	AODF670	Fine mode AOD at 670 nm
tau670_1	AODC670	Coarse mode AOD at 670 nm
tau865_0	AODF865	Fine mode AOD at 865 nm
tau865_1	AODC865	Coarse mode AOD at 865 nm
tau1020_0	AODF1020	Fine mode AOD at 1020 nm
tau1020_1	AODC1020	Coarse mode AOD at 1020 nm
ssa443	SSA443	Single Scattering Albedo at 443 nm
ssa490	SSA490	Single Scattering Albedo at 490 nm
ssa565	SSA565	Single Scattering Albedo at 565 nm
ssa670	SSA670	Single Scattering Albedo at 670 nm
ssa865	SSA865	Single Scattering Albedo at 865 nm
ssa1020	SSA1020	Single Scattering Albedo at 1020 nm
ssa443_0	SSAF443	Fine mode Single Scattering Albedo at 443 nm
ssa443_1	SSAC443	Coarse mode Single Scattering Albedo at 443 nm
ssa490_0	SSAF490	Fine mode Single Scattering Albedo at 490 nm
ssa490_1	SSAC490	Coarse mode Single Scattering Albedo at 490 nm
ssa565_0	SSAF565	Fine mode Single Scattering Albedo at 565 nm
ssa565_1	SSAC565	Coarse mode Single Scattering Albedo at 565 nm
ssa670_0	SSAF670	Fine mode Single Scattering Albedo at 670 nm
ssa670_1	SSAC670	Coarse mode Single Scattering Albedo at 670 nm
ssa865_0	SSAF865	Fine mode Single Scattering Albedo at 865 nm

ssa865_1	SSAC865	Coarse mode Single Scattering Albedo at 865 nm
ssa1020_0	SSAF1020	Fine mode Single Scattering Albedo at 1020 nm
ssa1020_1	SSAC1020	Coarse mode Single Scattering Albedo at 1020 nm
salbedo443	DHR443	Directional Hemispherical Reflectance at 443 nm
salbedo490	DHR490	Directional Hemispherical Reflectance at 490 nm
salbedo565	DHR565	Directional Hemispherical Reflectance at 565 nm
salbedo670	DHR670	Directional Hemispherical Reflectance at 670 nm
salbedo865	DHR865	Directional Hemispherical Reflectance at 865 nm
salbedo1020	DHR1020	Directional Hemispherical Reflectance at 1020 nm
chem_aer_relative_humidity_0	RH_F	Aerosol Fine Mode Relative Humidity
chem_aer_relative_humidity_1	RH_C	Aerosol Coarse Mode Relative Humidity
chem_aer_water_fraction_0	Water_Fraction_F	Fine Mode Water Fraction
chem_aer_water_fraction_1	Water_Fraction_C	Coarse Mode Water Fraction
chem_aer_soluble_fraction_0	Soluble_Fraction_F	Fine Mode Soluble Fraction
chem_aer_soluble_fraction_1	Soluble_Fraction_C	Coarse Mode Soluble Fraction
chem_aer_insoluble_fraction_0	Insoluble_Fraction_F	Fine Mode Insoluble Fraction
chem_aer_insoluble_fraction_1	Insoluble_Fraction_C	Coarse Mode Insoluble Fraction
chem_aer_soot_fraction_0	Soot_Fraction_F	Fine Mode Soot Fraction
chem_aer_soot_fraction_1	Soot_Fraction_C	Coarse Mode Soot Fraction
chem_aer_iron_fraction_0	Iron_Fraction_F	Fine Mode Iron Fraction
chem_aer_iron_fraction_1	Iron_Fraction_C	Coarse Mode Iron Fraction
chem_aer_brc_fraction_0	BrC_Fraction_F	Fine Mode BrC Fraction
chem_aer_brc_fraction_1	BrC_Fraction_C	Coarse Mode BrC Fraction
chem_aer_water_volume_concentration_0	Water_Volume_Concentration_F	Fine Mode Water Volume Concentration
chem_aer_soluble_volume_concentration_0	Soluble_Volume_Concentration_F	Fine Mode Soluble Volume Concentration
chem_aer_insoluble_volume_concentration_0	Insoluble_Volume_Concentration_F	Fine Mode Insoluble Volume Concentration
chem_aer_soot_volume_concentration_0	Soot_Volume_Concentration_F	Fine Mode Soot Volume Concentration
chem_aer_iron_volume_concentration_0	Iron_Volume_Concentration_F	Fine Mode Iron Volume Concentration
chem_aer_brc_volume_concentration_0	BrC_Volume_Concentration_F	Fine Mode BrC Volume Concentration
chem_aer_water_volume_concentration_1	Water_Volume_Concentration_C	Coarse Mode Water Volume Concentration
chem_aer_soluble_volume_concentration_1	Soluble_Volume_Concentration_C	Coarse Mode Soluble Volume Concentration
chem_aer_insoluble_volume_concentration_1	Insoluble_Volume_Concentration_C	Coarse Mode Insoluble Volume Concentration

chem_aer_soot_volume_concentration_1	Soot_Volume_Concentration_C	Coarse Mode Soot Volume Concentration
chem_aer_iron_volume_concentration_1	Iron_Volume_Concentration_C	Coarse Mode Iron Volume Concentration
chem_aer_brc_volume_concentration_1	BrC_Volume_Concentration_C	Coarse Mode BrC Volume Concentration

Table 4: POLDER GRASP/Components product specification.